Colombo Geographer

Journal of Colombo Geographer

Analyzing the Urban Heat Island Scenario Using Satellite Imagery: A Case Study of Matara Municipal Council

M.A.F. Afra[1], M.H.F. Nuskiya[1], Omala Perera[2], I.L.M. Zahir[1], Fareena Ruzaik[2]

[1]*Department of Geography, South Eastern University of Sri Lanka*
[2]*Department of Geography, University of Colombo, Sri Lanka*

Abstract

Urban Heat Island (UHI) is an increasingly prevalent phenomenon in rapidly urbanizing areas, resulting from the conversion of natural landscapes into impervious built-up surfaces, which absorb and retain more solar radiation than vegetated or natural environments. This study assesses the spatio-temporal dynamics of UHI within the Matara Municipal Council (MMC) area in Sri Lanka by analyzing changes in Land Surface Temperature (LST) between 2016 and 2024. Employing Landsat 8 satellite imagery, key indices such as LST, Normalized Difference Vegetation Index (NDVI), and Normalized Difference Built-up Index (NDBI) were derived following rigorous image pre-processing procedures. UHI intensity was quantified by calculating the temperature differential between urban and surrounding rural areas. The results indicate a marked increase in LST over the period, with the maximum LST rising by 3.69°C and the mean LST by 2.51°C, largely attributable to urban expansion and concomitant vegetation loss. Spatial analysis revealed that densely built-up zones exhibit elevated surface temperatures, whereas areas with higher vegetation density show significantly lower LST values, underscoring the mitigating influence of green cover. Correlation analyses confirmed a moderate negative association between LST and NDVI and a strong positive correlation between LST and NDBI, reinforcing the role of urban infrastructure in exacerbating surface heating. These findings emphasise the critical impact of urbanization on UHI intensification, which poses significant environmental and public health challenges, including increased energy demands for cooling and heightened pressure on water resources. The study advocates for the incorporation of green infrastructure and sustainable urban planning measures to alleviate UHI effects. Mapping the spatial distribution of UHI provides essential insights for policy interventions aimed at fostering resilient and climate-adaptive urban environments in Matara.

Keywords: Urban Heat Island, Land Surface Temperature, Preprocessing, Landscapes, Sustainable

1. Introduction

Temperature has been increasing in many parts of the world due to natural and anthropogenic activities. Urban Heat Island (UHI) is a crucial aspect of urban areas. Increasing Land Surface Temperature (LST) leads to the formation of an UHI in urban centres. Sri Lanka is a developing country with

Corresponding author.
E-mail address: nuskiyahassan@seu.ac.lk (M.H.F. Nuskiya)

a rapid urbanization process, which has gradually led to UHI in recent decades. However, LST frequently changes depending upon climatic conditions and other human activities, which makes its exact prediction a challenge. Urbanization contributes to increased greenhouse gas (GHG) emissions and alters natural landscapes, leading to significant climatic impacts at all scales. The transformation of land cover and the use of heat-retaining urban materials result in the re-emission of absorbed heat as long wave radiation at night, raising urban temperatures above those of surrounding rural areas (Thambawita et al., 2023; Zahir et al., 2024). In the 21st century, people faced one of the critical issues in UHI's aftermath due to urbanization and industrialization. Generally, built-up areas and LST are important phenomena in global climate change (Rajeshwari & Mani, 2014; Nuskiya et al., 2023). Air temperature in urban areas is significantly influenced by factors such as building geometry, the thermal and radiative properties of construction materials, and heat released from human activities like domestic heating, traffic, and industrial processes (Morales-Inzunza et al., 2023). This phenomenon, known as the UHI effect, describes the tendency of cities to be warmer than surrounding rural regions due to these anthropogenic influences.

In tropical cities, cloud contamination is a frequent issue in optical satellite data, such as the Landsat series, making long-term observation and analysis more challenging. With rapid population growth driving extensive urbanization in many tropical and subtropical regions, numerous administrative and planning challenges have emerged (Tombari, 2019). These challenges underscore the need for timely and accurate monitoring of large-scale urban development using satellite remote sensing technologies. Sri Lanka is undergoing rapid urbanization, with projections indicating that 60% of the population will be living in urban areas by 2030 (Pathiranage et al., 2018). The Colombo Metropolitan Area, a fast-growing urban center in South Asia, has been the focus of studies analysing spatial and temporal changes in LST (Ranagalage et al., 2017). In line with the global trend of rising temperatures, the country has experienced a significant increase in average annual surface temperatures over the past century (Sanjeewani & Manawadu, 2016; Hansen et al., 2010). However, the expansion of built-up areas and the removal of vegetation cover contributed to an increase in LST, leading to a rise in the UHI effect in urban areas (Tombari, 2019; Zahir et al., 2024). Urban vegetation and greenery play a vital role in mitigating the UHI effect (Zahir et al., 2024). Researchers have utilised Google Earth Engine (GEE) to analyze vegetation conditions, soil moisture, and temperature-related climate change effects (Nuskiya et al., 2024). Geospatial analysis and vegetation indices are essential tools for promoting urban sustainability and resilience (Zahir et al., 2024). The study also noted that the urban area is more vulnerable to increased urban heat due to reduced vegetation cover, while the village showed the least temperature variation (Jumari et al., 2023).

Understanding the microclimate of urban areas relies heavily on satellite-based geoinformatics techniques, which also play a crucial role in analyzing the effects of the UHI. Advancements in thermal remote sensing technology have significantly enhanced the study of UHI (Dousset et al., 2003; Li et al., 2012; Ranagalage et al., 2017). It highlights a significant temperature contrast between urban and rural areas, with urban regions exhibiting the highest temperatures. Advancements in satellite technology have enabled the acquisition of continuous surface data, offering greater coverage than traditional point-based observations for LST analysis. Tsou et al. (2017) conducted a study assessing the UHI effect using Landsat 8 imagery. The researchers applied various techniques to estimate LST, identifying the most effective algorithm for LST retrieval. Furthermore, the calculation of LST has been facilitated by digital image processing tools and satellite imagery. A study by Rajeshwari and Mani (2014), Landsat 8 OLI/TIRS data and the Split-Window (SW) technique to derive LST. The SW method incorporated Operational Land Imager (OLI) bands 2, 3, 4, and 5, along with the spectral radiance and emissivity of two Thermal Infrared (TIR) bands. It indicated lower LST in hilly regions due to dense vegetation cover and higher LST in arid zones. Furthermore, Landsat 8 OLI/TIRS data, when used in conjunction with the SW technique, enables LST analysis by incorporating Land Surface Emissivity (LSE) derived from the OLI and NIR bands and Brightness Temperature (BT) values from both thermal bands (Singh, 2017).

In addition, the study by Florim et al. (2021) investigates the UHI phenomenon by examining the relationships between LST, the Normalized Difference Vegetation Index (NDVI), and the Normalized Difference Built-up Index (NDBI). It offers valuable insights into the development and intensification of UHI, highlighting that vegetation cover mitigates heat accumulation, whereas built-up areas and exposed surfaces significantly contribute to it. The study also underscores that the presence of vegetation and water bodies was found to lower LST by creating cooler microclimates. However, identifying spatial patterns of UHI is essential for informing urban planning and implementing strategies to reduce adverse thermal impacts. Urban planners and decision-makers are therefore encouraged to use spatial data for effective heat mitigation (Florim et al., 2021).

The UHI effect is becoming increasingly prominent in underdeveloped and developing urban regions due to rapid population growth and unplanned urbanization. Thapa (2021) reported a notable increase in UHI intensity, underscoring the urgent need for public awareness, strategic planning, and intervention to address UHI in growing cities. Similarly, Malik et al. (2019) analyzed the interrelationships between LST, NDVI, and NDBI using Landsat 8 imagery for a watershed region. LST was retrieved from thermal bands to examine spatial and seasonal temperature variations. The study revealed that maximum temperatures occurred in urbanized or built-up areas, emphasising their heat-retaining characteristics. Understanding the interplay among LST, NDVI, and NDBI is critical for assessing climate change impacts on ecosystems and predicting vegetation health in watersheds. LST serves as a key parameter in climate studies, urban land-use planning, and thermal balance analysis. Anandababu et al. (2018) employed NDVI, derived from red and NIR bands, to evaluate vegetation dynamics. Their analysis indicated that areas with high NDVI values corresponded with lower LSTs, reinforcing the cooling effect of vegetation. Furthermore, Guha et al. (2018) explored the relationship between LST, NDVI, and NDBI by applying threshold values to distinguish land use types. It also highlights that built-up and bare land areas are directly associated with elevated LSTs, illustrating how urbanization influences surface thermal properties and land surface processes.

The primary cause of surface UHI formation is the reduction of vegetation due to poorly planned urban expansion, where green areas are replaced by impervious surfaces such as buildings, roads, and pavements. Rapid urbanization intensifies surface UHI effects. At this level, several factors contribute to the formation of the UHI effect in urban areas, including land use changes, reduced vegetation, and heat emitted from buildings and infrastructure that absorb and subsequently release heat into the environment. However, overheating is a concerning phenomenon that poses serious health risks, particularly for children, women, and the elderly. Therefore, this study aims to assess the UHI phenomenon between 2016 and 2024 and identify areas with elevated LST which are crucial for urban planners and policymakers in implementing heat reduction strategies. Promoting green cities can serve as an effective approach to mitigate heat-related impacts. Recognising the spatial patterns of surface UHI through mapping enables urban planning policies to address the adverse effects more effectively.

2. Materials and methods

2.1 Study Area

The study area, located in the Matara Municipal Council (MMC) in the Southern Province of Sri Lanka, is one of the country's prominent coastal cities. Geographically, it lies along the southern coastline between 5° 55' 54" – 5° 59'44 " latitude and 80° 30' 05" – 80° 37' 44" longitude, covering a total land area of approximately 1,283 km² (Figure 1). MMC experience a tropical rainforest climate due to its proximity to the equator, characterised by consistently high temperatures and rainfall throughout the year. The average annual temperature is 26.8°C, and the area receives about 2,147 mm of annual precipitation. Monthly temperature fluctuations range from an average minimum of 23°C to a maximum of 31.1°C. Rainfall is recorded throughout the year, with monthly averages ranging between 22 mm and 66 mm.

According to Sri Lanka's 2012 national census, the population within the study area increased by 40%, leading to the incorporation of 46 surrounding villages into the administrative boundaries. MMC was officially designated a municipality by the Urban Development Authority (UDA) in 2002. As a major commercial center on Sri Lanka's southern coast, the study area plays a significant role in driving regional development in the Southern Province (Pathiranage et al., 2018).

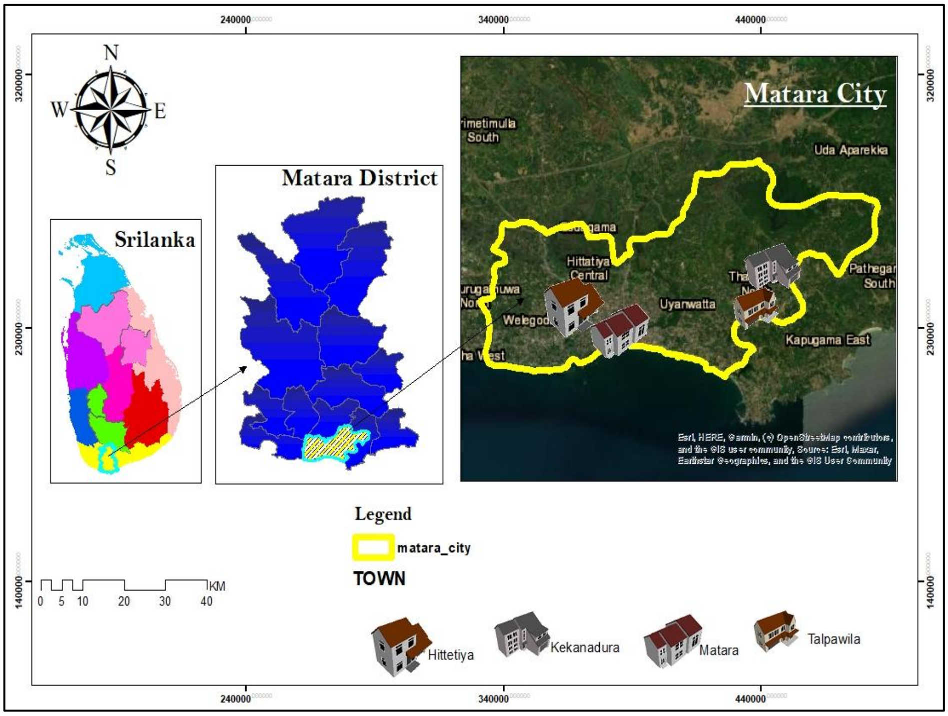

Figure 1: Location of Study Area

2.2 Materials

The primary data source for this study comprises satellite imagery obtained from the Landsat 8 OLI/TIRS data. These images were downloaded from the United States Geological Survey (USGS) Earth Explorer platform (https://earthexplorer.usgs.gov/), a widely recognized and reliable resource for remote sensing data, particularly in climate and environmental studies. The analysis focuses on two key dates: November 10, 2016, and January 17, 2024. The selected imagery maintains consistent path and row identifiers, enabling accurate temporal comparisons (Table 1). The cloud cover for the images was 1.51% and 4.10%, respectively, ensuring minimal atmospheric interference and high-quality data for analysis. This longitudinal dataset supports the evaluation of how urban expansion within the MMC area has influenced changes in LST over time.

Table 1: Source of Landsat 8 OLI/TIRS Data

Acquisition Date	Path/Row	Satellite/Sensor	Cloud Cover
2016.11.10	141/056	Landsat 8 OLI/TIRS	1.51
2024.01.17	141/056	Landsat 8 OLI/TIRS	4.10

The Landsat 8 sensor is equipped with multiple spectral bands, each designed for specific applications in remote sensing. Table 2 provides detailed information on these bands, including their descriptions, wavelength ranges, and spatial resolutions. This information is essential for analysing various land surface characteristics and vegetation properties, enabling more accurate environmental and climate assessments.

Table 2: Specification of the Bands of Landsat 8 OLI/TIRS

Band Name	Wavelength	Resolution
Band 1 Coastal Aerosol	0.43 - 0.45 µm	30 m
Band 2 Blue	0.45 - 0.51 µm	30 m
Band 3 Green	0.53 - 0.59 µm	30 m
Band 4 Red	0.64 - 0.67 µm	30 m
Band 5 Near-Infrared	0.85 - 0.88 µm	30 m
Band 6 SWIR 1	1.57 - 1.65 µm	30 m
Band 7 SWIR 2	2.11 - 2.29 µm	30 m
Band 8 Panchromatic (PAN)	0.50 - 0.68 µm	10 m
Band 9 Cirrus	1.36 - 1.38 µm	30 m

Source: https://www.usgs.gov/landsat-missions/landsat-8

2.3 Data Analysis

The initial step in the data analysis process involved image pre-processing to enhance the quality of the satellite imagery and enabling the extraction of meaningful features. This included geometric correction to ensure accurate spatial alignment, atmospheric correction to eliminate atmospheric distortions, and the conversion of thermal band data to surface reflectance. The preprocessed images were then analysed using ArcGIS software, which facilitated the integration and visualisation of the spatial data layer.

After the pre-processing of satellite images, key indices were calculated to evaluate urban heat dynamics. LST was evaluated using a proposed approach designed to process Landsat 8 imagery. These products were first geometrically corrected, and the initial step of the methodology involved converting the Digital Number (DN) values of Band 10 to Top of Atmosphere (TOA) spectral radiance at the sensor level using Eq. 1 (Teixeira Pinto et al., 2020).

$$\mathrm{L}\lambda = \frac{(\mathrm{L}max - \mathrm{L}min) * \mathrm{Qcal}}{(Qcalmax - Qcalmin)} + \mathrm{L}min - \mathrm{O}i \qquad \text{(Eq. 1)}$$

where, Lmax - the maximum radiance (Wm-2sr-1µm-1); Lmin - the minimum radiance (Wm-2sr-1µm-1); Qcal - the DN value of pixel; Qcalmax - the maximum DN value of pixels; Qcalmin - the minimum DN value of pixels; Oi - the correction value for band 10.

After converting the DN values to at-sensor spectral radiance, the TIRS band data were further converted into BT using the thermal constants provided in the metadata file and Eq. 2 (Masiello et al., 2013):

$$\mathrm{BT} = \frac{K2}{In\left(\frac{K1}{L\lambda}\right) + 1} - 273.15 \qquad \text{(Eq. 2)}$$

where, BT - TOA brightness temperature (°C); Lλ - TOA spectral radiance (Watts/(m2 * sr * µm)); K1 - Constant Band (No.); K2 - Constant Band (No.).

The K1 and K2 constants are obtained from the thermal coefficients of TIRS band 10, as specified in the metadata file associated with the satellite image. To express the resulting temperatures in degrees Celsius, a correction is applied by subtracting absolute zero, approximately equal to -273.15°C. Given that the study area has relatively dry atmospheric conditions with minimal variation in water vapour content, atmospheric effects were not considered in the retrieval of LST.

However, the calculation of the NDVI (Eq. 3) is essential for deriving Proportional Vegetation (Pv) (Eq. 4) and LSE (ε) (Neinavaz et al., 2020; Zahir et al., 2024).

$$NDVI = \frac{(NIR - Red)}{(NIR + Red)} \qquad \text{(Eq. 3)}$$

where, Red – Band 4; NIR – Band 5

$$v = \left(\frac{\text{NDVI}-\text{NDVI}min}{\text{NDVI}max-\text{NDVI}min}\right)^2 \quad \text{(Eq. 4)}$$

where, Pv - Proportion of Vegetation; NDVI - DN values from NDVI Image; NDVImin -Minimum DN values from NDVI Image; NDVImax - Maximum DN values from NDVI Image.

The calculation of LSE is essential for accurately estimating LST, as LSE serves as a proportionality factor that adjusts blackbody radiance to account for the actual emitted radiance (Eq. 5). It represents the surface's ability to transmit thermal energy into the atmosphere (Kruse et al., 1993). At the pixel level, natural surfaces exhibit heterogeneity in LSE due to variations in surface characteristics. LSE is highly influenced by factors such as surface roughness and the type and density of vegetation cover (Barsi et al., 2014). It is typically derived from NDVI values as the average emissivity of specific surface elements.

E = 0.004 * PV + 0.986 (Eq. 5)

where, E - LSE; Pv - Proportion of Vegetation

Finally, the Estimated Surface Temperature (EST), also referred to as LST, was calculated as the radiative temperature using the TOA brightness temperature, the wavelength of emitted radiance, and LSE, as outlined in Eq. 6 (Kumar et al., 2022). In remote sensing and geospatial studies, EST is commonly used interchangeably with LST and represents the temperature of the Earth's surface derived from satellite-based TIR data.

$$LST = \frac{BT}{1+\left(\frac{\lambda.BT}{\rho}\right)In(\varepsilon)} \text{-273.15} \quad \text{(Eq. 6)}$$

Where, λ - wavelength of emitted radiance (~10.895 µm for Landsat 8 Band 10); ρ -1.438×10−2 m; Subtract 273.15 to convert from Kelvin to Celsius.

Ultimately, the UHI effect refers to the phenomenon in which urban areas experience higher temperatures than surrounding rural regions, primarily due to human activities and modifications to the natural environment. To quantify this effect, the most widely used approach involves calculating the difference in LST between urban and rural areas (Eq. 8). This temperature differential serves as an indicator of UHI intensity.

$$\text{UHI} = \text{LST}urban - \text{LST}rural \qquad \text{(Eq. 7)}$$

where, LSTurban - Average LST in urban/built-up areas; LSTrural - Average LST in surrounding rural/natural areas

The NDBI is a remote sensing index commonly used to identify and map built-up areas in satellite imagery. It is particularly valuable in urban studies for assessing the extent of impervious surfaces, such as buildings, roads, and other man-made structures (Slonecker et al., 2001). NDBI plays a significant role in identifying urban areas, analysing their correlation with LST, mapping UHI zones, and supporting urban planning strategies. The index is calculated using Eq. 8.

$$\text{NDBI} = \frac{(\text{SWIR} - \text{NIR})}{(\text{SWIR} + \text{NIR})} \qquad \text{(Eq. 8)}$$

where, SWIR - Short-Wave Infrared band (e.g., Band 6 for Landsat 8); NIR band (e.g., Band 5 for Landsat 8)

3. Results & Discussions

The results of the LST analysis reveal the spatial distribution of temperature changes within the MMC area between 2016 and 2024. The analysis highlights trends in LST and establishes correlations with patterns of urbanization and vegetation cover, offering valuable insights into the intensity and progression of the UHI effect in the region. The analysis presented in Figures 2 and 3 illustrates the LST distribution for the study area in the years 2016 and 2024. Both maps show LST values ranging from 26°C to 30°C; however, between 2016 and 2024, the maximum LST increased by 3.69°C, while the minimum and mean LST rose by 2.48°C and 2.51°C, respectively. Spatially, the central region of the study area, characterised by dense urban development, exhibits the highest LST values. In contrast, the northern and northeastern regions, which consist largely of less urbanized or vegetated areas, display relatively lower LSTs. This consistent increase in LST values indicates an intensification of the UHI effect, likely due to urban expansion and reduced vegetation cover.

Similarly, the NDVI reveals noticeable changes in vegetation cover over the eight years, where the maximum NDVI increased slightly, while the minimum NDVI decreased, and the mean NDVI showed a marginal increase of 0.0106. The most significant decline in NDVI values is observed in the central parts of MMC, primarily due to the expansion of built-up areas and the consequent loss of vegetation. NDVI serves as a key indicator for assessing vegetation distribution across the city. While overall vegetation cover in MMC remains limited, notable vegetated zones are found in areas such as Kekanadura North, Kekanadura Central, and Deeyagaha East. Although urbanization expanded, the slight increase in mean NDVI may be due to localized greening efforts or vegetation growth in peripheral areas. Nonetheless, the overall vegetative health appears relatively stable, with limited but positive change.

The maximum NDBI value increased from 0.218 to 0.276, suggesting a 5.8% increase in built-up intensity, while the mean NDBI slightly increased by 0.007 in study period. The results indicate a notable increase in built-up areas over the eight-year period, driven largely by population growth and subsequent urban expansion. These changes confirm the expansion of urban infrastructure, especially in central Matara, aligning with the observed increase in LST. This spatial pattern underscores the ongoing transformation of land cover from vegetated to impervious surfaces, contributing to the growth of urban infrastructure.

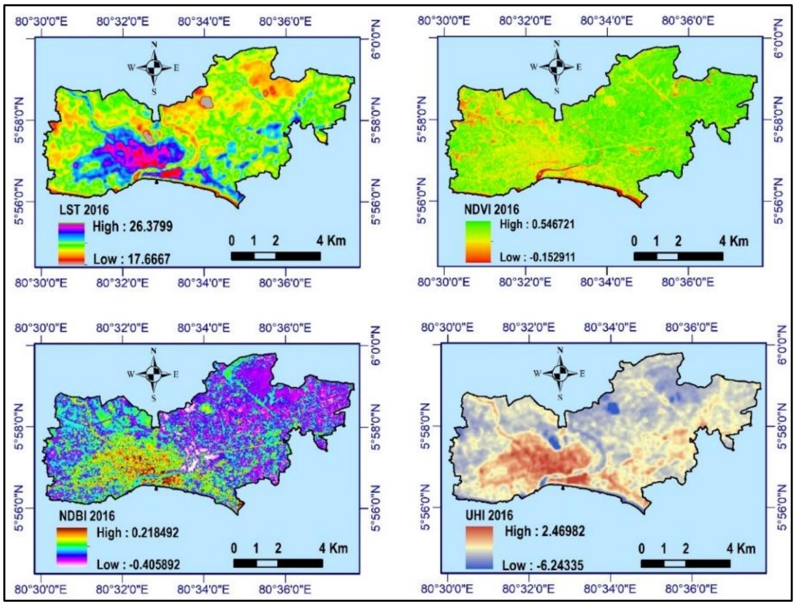

Figure 2: LST, NDVI, NDBI and UHI in 2016

The concurrent increase in LST and NDBI, alongside the slight rise in NDVI, highlights the significant influence of urbanization on surface temperature patterns (Table 3). These results indicate a clear upward trend in LST throughout the MMC area, primarily driven by continuous urban expansion and the reduction of vegetative cover. The findings emphasize the urgent need for sustainable urban planning interventions, particularly the protection and enhancement of urban green spaces, to effectively mitigate the intensifying UHI effect in the region.

Table 3: LST, NDBI, and NDVI values in 2016 and 2024

Year	Max LST (°C)	Min LST (°C)	Mean LST (°C)
2016	26.37	17.66	22.71
2024	30.06	20.14	25.22
+/-	3.69	2.48	2.51
	Max NDBI	Min NDBI	Mean NDBI
2016	0.218	-0.405	-0.185
2024	0.276	-0.404	-0.178
+/-	0.058	0.001	-0.017
	Max NDVI	Min NDVI	Mean NDVI
2016	0.546	-0.152	0.3354
2024	0.588	-0.191	0.3460
+/-	0.042	-0.049	0.0106

The statistical analysis of the pairwise relationships among LST, NDVI, and NDBI for the years 2016 and 2024 reveals notable trends. In the 2016 correlation matrix, the relationship between LST and NDVI shows a correlation coefficient of -0.32, indicating a weak to moderate negative correlation. This suggests that areas with higher vegetation cover tend to have lower land surface temperatures, highlighting the cooling effect of green spaces. In contrast, the correlation between LST and NDBI is 0.58, reflecting a moderate positive correlation, which implies that built-up areas are associated with increased LST, aligning with the UHI effect. Furthermore, the correlation between NDVI and NDBI is -0.66, indicating a strong negative correlation. This confirms that vegetation and built-up areas are spatially inverse, where urban expansion typically reduces vegetative cover.

Similarly, in 2024, a moderate negative correlation (r = -0.45) between LST and NDVI indicates that areas with greater vegetation cover tend to exhibit lower LSTs. This supports the premise that vegetated areas help mitigate urban heat.

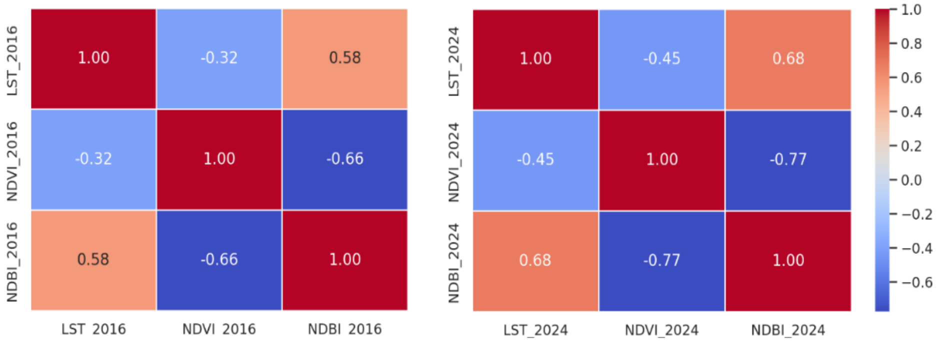

Figure 3: Correlation Matrix among LST, NDVI, and NDBI in 2016 and 2024

Conversely, a strong positive correlation (r = 0.68) between LST and NDBI suggests that increased built-up or impervious surfaces are associated with higher LST, highlighting the contribution of urbanization to the UHI effect. Additionally, a strong negative correlation (r = -0.77) between NDVI and NDBI demonstrates that urban expansion often leads to a reduction in vegetation cover (Figure 5).

A comparative analysis between 2016 and 2024 reveals a significant increase in UHI intensity. Several areas, including Weliweriya East, Kadeweediya East, Isadeen Town, Hittatiya West, Kotuwegoda North, and Weliweriya West, exhibit notably higher UHI values due to expanded urban development. The study of the relationships between LST, NDVI, and NDBI provides critical insight into identifying UHI patterns and estimating accurate LST values. Correspondingly, linear regression analysis shows a negative correlation between LST and NDVI, and a positive correlation between LST and NDBI. This indicates that built-up areas generally experience higher LSTs, while areas with dense vegetation show lower temperatures due to the cooling effect of vegetation and its ability to absorb CO_2. Consequently, many cities have adopted greening initiatives to mitigate rising temperatures.

However, the ongoing conversion of forests into built-up areas has become a widespread phenomenon, contributing to shifts in climatic conditions and increased temperatures. Areas with the highest LSTs are often the focal points of UHI formation. The urban heat island effect poses a serious environmental and public health risk, driven by the concentration of buildings, roads, and infrastructure that consume energy and trap heat.

Increased heat levels lead to higher energy demands for cooling and place pressure on water resources, especially impacting those involved in primary economic activities such as agriculture. Moreover, rapid changes in temperature and weather patterns are difficult for many urban residents to adapt to, heightening the vulnerability of urban populations to climate-related stress. Comparison between 2016 and 2024, the UHI value has increased incredibly. Some of the study areas including Weliweriya East, Kadeweediya East, Isadeen Town, Hittatiya West, Kotuwegoda North, and Weliweriya West have a higher UHI value due to increased urban area. The study of the relationship LST between NDBI and NDVI helps to recognise that indicators of urban heat islands, moreover assist in determining the correct value of LST. The linear regression analysis results in positive and negative relations between LST with NDVI and NDBI. Mostly built-up areas comprise a higher value of LST than the surrounding areas. Where vegetation cover is located, that shows a low rate of LST because vegetation cover absorbs CO_2. Therefore, many cities are planted with greenery. Converting forests into built-up areas is a common thing in each region; on the other hand, climatic conditions are changed by this function temperature will be changed. Where the highest LST occurs, ition is prone to form UHI, which is a significant risk factor in urban areas. The concentration of buildings, roads, and other infrastructure and the replacement of vegetation require energy consumption, which absorbs and retains heat. Overheating demands higher electricity for cooling, and a water supply has health implications for residents. Especially, those who rely on primary economic activity, will be affected by the requirement for more water supply for crop production. Many people cannot bear the overheated environment in urban areas because sudden changes in weather patterns cannot be easily adapted to by those who survive in the city.

4. Conclusion

LST plays a crucial role in influencing climatic conditions and helps in identifying the spatial distribution of UHI. This study assessed the UHI trends in MMC for the years 2016 and 2024. Results show that built-up areas and bare land surfaces exhibit significantly higher surface temperatures, while vegetated zones maintain lower temperatures. However, MMC lacks substantial green cover within its urban core, although the surrounding rural and suburban regions possess relatively dense vegetation.

The rise in both LST and NDBI indicates ongoing urban expansion within the study area. This trend is largely driven by population growth and the resulting increase in infrastructure, such as buildings and roads which are key contributors to UHI formation. The intensification of UHI poses risks to human health and well-being, which can be mitigated through proper urban planning and the promotion of green infrastructure.

Several tactical actions are suggested in order to successfully reduce the UHI effect in the Matara Municipal Council area. First, LST can be considerably decreased by creating parks, gardens, and trees to increase vegetation. By acting as a carbon sink, encouraging evapotranspiration, and providing shade, vegetation helps to improve air quality and create cooler urban microclimates. Second, by reflecting sunlight, cool roofing materials and light-colored pavements can reduce heat absorption and subsequently lower surface temperatures. These materials are successful in preventing UHI, despite the fact that their initial costs may be higher. Thirdly, encouraging compact urban growth, mixed land use, and pedestrian-friendly infrastructure can help lower building energy use and vehicle emissions, which will help cool cities even more. Another important factor is public awareness; informing people about the origins and effects of UHI, as well as the advantages of lowering LST, can promote environmental stewardship and community involvement. Furthermore, the creation and implementation of urban policies that prioritise green infrastructure and environmental sustainability are essential for directing future land use, vegetation management, and construction. Lastly, adding more greenery improves the aesthetic appeal of urban areas and lowers LST, which may draw tourists who appreciate varied and natural urban landscapes.

References

Alhawiti, R. H., & Mitsova, D. (2016). Using Landsat-8 data to explore the correlation between urban heat island and urban land uses. *IJRET: International Journal of Research in Engineering and Technology, 5*(3), 457–466.

Anandababu, D., Purushothaman, B. M., & Suresh, B. S. (2018). Estimation of land surface temperature using Landsat 8 data. *International Journal of Advance Research, 4*(2), 177–186.

Barsi, J. A., Schott, J. R., Hook, S. J., Raqueno, N. G., Markham, B. L., & Radocinski, R. G. (2014). Landsat-8 thermal infrared sensor (TIRS) vicarious radiometric calibration. *Remote Sensing, 6*(11), 11607–11626.

Dousset, B., & Gourmelon, F. (2003). Satellite multi-sensor data analysis of urban surface temperatures and landcover. *ISPRS Journal of Photogrammetry and Remote Sensing, 58*, 43–54.

Florim, I., Albert, B., & Shpejtim, B. (2021). Measuring UHI using Landsat 8 OLI and TIRS data with NDVI and NDBI in Municipality of Prishtina. *Disaster Advances, 14*, 25–36.

Guha, S., Govil, H., Dey, A., & Gill, N. (2018). Analytical study of land surface temperature with NDVI and NDBI using Landsat 8 OLI and TIRS data in Florence and Naples city, Italy. *European Journal of Remote Sensing, 51*(1), 667–678.

Hansen, J., Ruedy, R., Sato, M., & Lo, K. (2010). Global surface temperature change. *Reviews of Geophysics, 48*(4).

Jabbar, H. H., Mustafa, & Al-Hameedawi, A. (2023). Urban heat islands: A review of contributing factors, effects, and data. *IOP Conference Series: Earth and*

Environmental Science, *1129*, 012038. https://doi.org/10.1088/1755-1315/1129/1/012038

Jumari, N. A. S. K., Ahmed, A. N., Huang, Y. F., Ng, J. L., Koo, C. H., Chong, K. L., ... & Elshafie, A. (2023). Analysis of urban heat islands with Landsat satellite images and GIS in Kuala Lumpur Metropolitan City. *Heliyon*, *9*(8).

Kruse, F. A., Lefkoff, A. B., Boardman, J. W., Heidebrecht, K. B., Shapiro, A. T., Barloon, P. J., & Goetz, A. F. (1993). The spectral image processing system (SIPS)—interactive visualization and analysis of imaging spectrometer data. *Remote Sensing of Environment*, *44*(2–3), 145–163.

Kumar, D., Soni, A., & Kumar, M. (2022). Retrieval of land surface temperature from Landsat-8 thermal infrared sensor data. *Journal of Human, Earth, and Future*, *3*(2), 159–168.

Li, Y. Y., Zhang, H., & Kainz, W. (2012). Monitoring patterns of urban heat islands of the fast-growing Shanghai metropolis, China: Using time-series of Landsat TM/ETM+ data. *International Journal of Applied Earth Observation and Geoinformation*, *19*, 127–138.

Malik, M. S., Shukla, J. P., & Mishra, S. (2019). Relationship of LST, NDBI, and NDVI using Landsat-8 data in Kandaihimmat watershed, Hoshangabad, India.

Masiello, G., Serio, C., De Feis, I., Amoroso, M., Venafra, S., Trigo, I. F., & Watts, P. (2013). Kalman filter physical retrieval of surface emissivity and temperature from geostationary infrared radiances. *Atmospheric Measurement Techniques*, *6*, 3613–3634. https://doi.org/10.5194/amt-6-3613-2013

Morales-Inzunza, S., González-Trevizo, M. E., Martínez-Torres, K. E., Luna-León, A., Tamayo-Pérez, U. J., Fernández-Melchor, F., & Santamouris, M. (2023). On the potential of cool materials in the urban heat island context: Scalability challenges and technological setbacks towards building decarbonization. Energy and Buildings, 296, 113330. https://doi.org/10.1016/j.enbuild.2023.113330

Nanayakkara, S., Wang, W.-M., Cao, J., Wang, J., Zhou, W., & Weiqi. (2023). Analysis of urban heat island effect, heat stress and public health in Colombo, Sri Lanka and Shenzhen, China. Atmosphere, 14, 839. https://doi.org/10.3390/atmos14050839

Neinavaz, E., Skidmore, A. K., & Darvishzadeh, R. (2020). Effects of prediction accuracy of the proportion of vegetation cover on land surface emissivity and temperature using the NDVI threshold method. *International Journal of Applied Earth Observation and Geoinformation*, *85*, 101984.

Nuskiya, M. H. F., Zahir, I. L. M., Mohamed Thariq, M. G., Thennakoon, S., Iyoob, A. L., & Ameer, M. L. F. (2023). Spatiotemporal analysis of MODIS-based land surface temperature using Google Earth Engine (GEE) in Ampara District. In *Proceedings of the 14th International Conference on Sustainable Built Environment - 2023*, Kandy, Sri Lanka.

Nuskiya, M. H. F., Zahir, I. L. M., Rinos, M. H. M., & Iyoob, A. L. (2024). Assessing the impact of drought events through remote sensing based soil moisture analysis with Google Earth Engine in North Central Province, Sri Lanka. *Proceedings of the 8th International Conference on Climate Change 2024 (ICCC 2024)*.

Pathiranage, I. S., Kantakumar, L. N., & Sundaramoorthy, S. (2018). Remote sensing data and SLEUTH urban growth model: As decision support tools for urban planning. *Chinese Geographical Science, 28*, 274–286.

Rajeshwari, A., & Mani, N. D. (2014). Estimation of land surface temperature of Dindigul district using Landsat 8 data. *International Journal of Research in Engineering and Technology, 3*(5), 122–126.

Ranagalage, M., Estoque, R. C., & Murayama, Y. (2017). An urban heat island study of the Colombo metropolitan area, Sri Lanka, based on Landsat data (1997–2017). *ISPRS International Journal of Geo-Information, 6*(7), 189. https://doi.org/10.3390/ijgi6070189

Sanjeewani, R. M., & Manawadu, L. (2017). Spatial trends of land surface temperature variation over selected urban regions in Sri Lanka using remote sensing. *Asian Journal of Geoinformatics, 16*(3).

Singh, V. (2017). Estimating land surface temperature in ArcGIS using Landsat-8, Hoshangabad district, (Madhya Pradesh). *International Journal of Advanced Research, 3*(6), 1374–1379.

Slonecker, E. T., Jennings, D. B., & Garofalo, D. (2001). Remote sensing of impervious surfaces: A review. *Remote Sensing Reviews, 20*(3), 227–255.

Teixeira Pinto, C., Jing, X., & Leigh, L. (2020). Evaluation analysis of Landsat Level-1 and Level-2 data products using in situ measurements. *Remote Sensing, 12*(16), 2597. https://doi.org/10.3390/rs12162597

Thambawita, T. K. C. N., Munasinghe, D. S., & Yapa, L. K. K. (2023). Identification of urban heat island effect on land use land cover changes. *Journal of Geospatial Surveying, 3*(2), 43–53. https://doi.org/10.4038/jgs.v3i2.50

Thapa, P. (2021). Urban heat island analysis using Landsat 8 satellite data. In *11th International Geographic Information Science Conference* (pp. 1–16).

Tombari, B. (2019). Rapid urbanisation: Theories, causes, consequences and coping strategies. *Journal of Humanities and Social Sciences, 2*(3), 32–45. https://doi.org/10.22259/2642-9136.0203005

Tsou, J., Zhuang, J., Li, Y., & Zhang, Y. (2017). Urban heat island assessment using the Landsat 8 data: A case study in Shenzhen and Hong Kong. *Urban Science, 1*(1), 10.

Zahir, I. L. M., Nuskiya, M. H. F., Sangasumana, V. P., Iyoob, A. L., & Ameer, M. L. F. (2024). Monitoring urban green space using remote sensing derived-vegetation indices in Colombo District, Sri Lanka. *Procedia Computer Science, 236*, 248–256.

Zahir, I. L. M., Thennakoon, S., Sangasumana, R. P., Herath, J., Madurapperuma, B., & Iyoob, A. L. (2021). Spatiotemporal land-use changes of Batticaloa Municipal Council in Sri Lanka from 1990 to 2030 using Land Change Modeler. *Geographies, 1*(3), 166.